HHS Public Access

Author manuscript

AJR Am J Roentgenol. Author manuscript; available in PMC 2021 March 04.

Published in final edited form as:

AJR Am J Roentgenol. 2016 July ; 207(1): 205–216. doi:10.2214/AJR.15.15873.

Performance of DWI as a Rapid Unenhanced Technique for Detecting Mammographically Occult Breast Cancer in Elevated-Risk Women With Dense Breasts

Elizabeth S. McDonald[1,2], **Jill A. Hammersley**[1], **Shinn-Huey S. Chou**[1], **Habib Rahbar**[1], **John R. Scheel**[1], **Christoph I. Lee**[1], **Cheng-Liang Liu**[1], **Constance D. Lehman**[1], **Savannah C. Partridge**[1]

[1]Department of Radiology, University of Washington, Seattle Cancer Care Alliance, 825 Eastlake Ave E, Rm G3-200, Seattle, WA 98109-1023

[2]Present address: Department of Radiology, Perelman School of Medicine, University of Pennsylvania, Philadelphia, PA.

Abstract

OBJECTIVE.—The objective of our study was to evaluate the performance of DWI to detect mammographically occult breast cancer in elevated-risk women with dense breasts.

MATERIALS AND METHODS.—We retrospectively reviewed all women who underwent screening breast MRI at our institution from January 2007 through May 2013. We created a case-control cohort composed of 48 subjects with mammographically dense breasts: 24 with mammographically occult cancer detected on MRI and 24 healthy women with negative MRI findings who were matched to the subjects with breast cancer patients for age, breast density, and MRI protocol. The contrast-to-noise ratio (CNR), apparent diffusion coefficient (ADC), and conspicuity score (range, 1–5) were assessed on DWI for all malignancies. Lesions and normal tissue were compared using the Wilcoxon signed rank test; associations with clinical characteristics were evaluated using the Mann-Whitney *U* test. Three experienced breast imagers who were blinded to medical records and contrast-enhanced MRI findings independently evaluated the unenhanced MRI scans of the 48 women for the presence of cancer.

RESULTS.—Mammographically occult breast cancers (invasive carcinoma, $n = 16$; ductal carcinoma in situ, $n = 8$) in women with dense breasts typically exhibited higher signal intensity on DWI than normal parenchyma (median CNR of cancers, 1.4; median conspicuity score of cancers, 4) and a lower ADC (median, 1.31 vs 1.79×10^{-3} mm^2/s, respectively) ($p < 0.0001$). The conspicuity score, CNR, and ADC were not associated with patient age, menopausal status, lesion size, morphologic type, or histology ($p > 0.05$). Average reader performance using unenhanced MRI was 45% sensitivity, 91% specificity, 62% positive predictive value, and 83% negative predictive value.

Address correspondence to S. C. Partridge (scp3@u.washington.edu).

Based on presentations at the ARRS 2014 Annual Meeting, San Diego, CA, and at the International Society for Magnetic Resonance in Medicine 2015 annual meeting, San Francisco, CA.

CONCLUSION.—In elevated-risk women with dense breasts, DWI can reveal cancers in addition to those detected on mammography alone with a low false-positive rate; these results suggest that DWI may have potential as a rapid supplemental screening tool.

Keywords

breast cancer screening; cancer detection; dense breasts; DWI; mammographically occult cancer; MRI; reader performance

MRI is recommended by the American Cancer Society as an adjunct screening modality to mammography in the high-risk population, defined as women with a lifetime risk of developing breast cancer of greater than 20% [1]. Most commonly, breast MRI is performed using a dynamic contrast-enhanced (DCE) technique, which has proven to be highly sensitive for the detection of breast cancer [2]. Independent of other risk factors, women with dense breasts on screening mammography have 1.5 times increased risk of developing breast cancer [3–5]; however, this risk factor alone currently does not qualify them for yearly screening by DCE-MRI. Furthermore, the sensitivity of screening mammography for the detection of breast cancer decreases as breast density increases [6]. As of September 2015, 24 states in the United States require that women with dense breasts be notified of their breast density, the associated increased cancer risks, and the associated limitations of screening mammography. However, there currently is no clear consensus about the optimal supplemental screening for these women [7,8]. A validated, safe, and cost-effective screening method is needed to detect mammographically occult cancers in women with dense breasts.

DWI is a short (2–3 minutes) unenhanced MRI technique that has shown promise for the detection and characterization of breast cancer [9]. DWI reveals the microscopic cellular environment and can show differences between normal breast tissue and malignant breast tissue without the aid of IV gadolinium [10]. Many mammographically and clinically occult breast cancers detected on DCE-MRI are also visible on DWI and can be differentiated from benign breast lesions on the basis of calculated apparent diffusion coefficients (ADCs) [11]. Accordingly, DWI has been proposed as an alternative to conventional contrast-enhanced MRI for supplemental screening of women with dense breasts because it avoids the safety and cost issues associated with gadolinium injection and the longer scanning time associated with DCE-MRI.

The use of unenhanced MRI with DWI for supplemental breast cancer screening is still in the early stages of investigation, with only a few published reports to date [12–14]. Breast DWI techniques currently are not standardized and lack a uniform method of interpretation, which limits widespread use. Nevertheless, preliminary studies have yielded promising results: One reader study of asymptomatic women showed a higher sensitivity of unenhanced DWI and T2-weighted MRI for detecting malignancy than mammography alone [14]. To our knowledge, none of the prior studies specifically investigated DWI for screening women with dense breasts and therefore the added value of unenhanced MRI to mammography for detecting cancer in this population is not clear. Thus, our goal was to assess the potential ability of DWI to reveal mammographically occult cancer in women

with dense breasts and to elucidate patient and imaging factors that may impact lesion conspicuity. In this study, we conducted a blinded reader study to assess performance characteristics for screening women with dense breasts using unenhanced MRI and performed unblinded evaluations of the DWI features of mammographically occult cancers.

Materials and Methods

Our study was approved by our institutional review board (IRB) and was HIPAA-compliant. The need to obtain informed consent was waived for this retrospective analysis. Consecutive screening breast MRI examinations performed from January 2007 through May 2013 were reviewed. During the study period, DWI was performed as part of the standard clinical breast MRI protocol. Eligible subjects were women who were 18 years old or older, were asymptomatic at the time of MRI, and had a recent mammographic density assessment (i.e., within 12 months of MRI) of heterogeneously dense or extremely dense breast tissue.

The MRI examinations were interpreted prospectively by one of six fellowship-trained breast imagers using the American College of Radiology (ACR) BI-RADS Breast MRI Lexicon [15]. The MRI examination findings, along with other patient characteristics including mammographic breast density, were entered into an established institutional breast MRI database. The outcomes for the study were obtained from the Consortium Oncology Data Integration (CODI) Project, which is an IRB-approved solid tumor clinical research database developed and maintained at our institution. Data sources for CODI include the breast MRI database; the institutional pathology database; and the regional Cancer Surveillance System tumor registry, which is part of the National Cancer Institute's Surveillance, Epidemiology, and End Results program. Additional information, including mammographic findings, breast cancer risk factors, and lesion histologic characteristics, was obtained from the medical records of the study subjects.

Subjects

Over the study period (January 2007–May 2013), 1069 women with heterogeneously dense or extremely dense breast tissue underwent breast MRI for screening at our institution, and mammographically occult breast cancer that was assessed as MRI BI-RADS category 4 or 5 was detected in 28 women. One subject had an additional ipsilateral breast cancer that was not mammographically occult, so that woman was excluded to avoid a confounding factor in the blinded reader study. Three women were excluded because DWI was not performed or the archived images were incomplete. Thus, 24 women with dense breast tissue who had mammographically occult breast cancers were included in the case-control study. One-to-one matching was achieved by randomly selecting a patient with negative or benign findings for each cancer case and matching the control subject to the cancer patient for age, breast density, and MRI protocol. Potential control subjects were identified from 811 women with heterogeneously dense or extremely dense breast tissue who underwent breast MRI for screening over the study period and who had negative or benign (BI-RADS category 1 or 2) clinical breast MRI interpretations and no breast cancer diagnosis within 12 months after MRI.

Image quality requirements for DWI scans were adequate whole-breast coverage including the mammographically occult lesion and adequate fat suppression (i.e., no complete technical failures). No cases were excluded from the study on the basis of these criteria.

MIR

Two clinical MRI protocols were used over the study time frame. Both protocols followed the guidelines established by the ACR breast MRI accreditation program [16] and included the following sequences in the following order: non-fat-suppressed T1-weighted, fat-suppressed T2-weighted, T1-weighted DCE-MRI, and DWI sequences performed in the axial orientation.

Before February 2010, imaging was performed on a 1.5-T scanner (Signa, GE Healthcare) with a dedicated 8-channel breast coil (High Definition, GE Healthcare or Sentinelle, Invivo) as previously described [11, 17]. Briefly, T2-weighted imaging was performed with a fat-suppressed 2D fast spin-echo (FSE) sequence with TR/TE of 6050/85, FOV of 32–38 cm, matrix size of 320 × 224, slice thickness of 1.6 mm, gap of 0 mm, and scanning time of 2 minutes 44 seconds. T1-weighted imaging was performed with a 3D fast spoiled gradient-recalled echo sequence with parallel imaging (Volume Imaging for Breast Assessment [VIBRANT], GE Healthcare) with TR/TE of 6.2/3, flip angle of 10°, FOV of 32–38 cm, matrix size of 420 × 420, and slice thickness of 1.6 mm. For the non-fat-suppressed T1-weighted sequence, the scanning time was 1 minute 31 seconds. For the fat-suppressed DCE-MRI sequence, the scanning time was 2 minutes 53 seconds per acquisition. Gadolinium contrast material (gadodiamide [Omniscan, GE Healthcare]) was power-injected after the first acquisition (0.1 mmol/kg of body weight administered at 2 mL/s and followed by a 20-mL saline flush), and three contrast-enhanced acquisitions were performed. DWI was performed using an echo-planar DWI sequence with parallel imaging (Array Spatial Sensitivity Encoding Technique [ASSET], GE Healthcare) and fat suppression (Spectral Inversion at Lipid [SPECIAL], GE Healthcare), reduction factor of 2, TR/TE of 7000/71.5, 3 signal averages, FOV of 36 × 36 cm, matrix size of 192 × 192, 25–28 slices, slice thickness of 5 mm, and gap of 0 mm. Diffusion gradients were applied in six directions with diffusion sensitizations (b values) of 0 and 600 s/mm^2; the scanning time was 2 minutes 40 seconds.

From February 2010 through May 2013, imaging was performed on a 3-T scanner (Achieva, Philips Healthcare) with a dedicated 16-channel breast coil (MammoTrak, Philips Healthcare) as previously described [18, 19]. Briefly, a fat-suppressed 2D FSE T2-weighted sequence was performed with a TR/TE of 5000/60, FOV of 22 × 33 cm, matrix size of 280 × 420, slice thickness of 1.3 mm, gap of 0 mm, and scanning time of 5 minutes 15 seconds. Non-fat-suppressed T1-weighted imaging was performed using a 3D fast gradient-echo sequence with TR/TE of 5.2/2.3, flip angle of 10°, FOV of 22 × 33 cm, matrix size of 440 × 660, slice thickness of 1.3 mm, and scanning time of 1 minute 52 seconds. DCE-MRI was performed using a fat-suppressed 3D fast gradient-echo sequence (Enhanced T1 High Resolution Isotropic Volume Excitation [eTHRIVE], Philips Healthcare) with TR/TE of 5.9/3.1, flip angle of 10°, FOV of 22 × 33 cm, matrix size of 440 × 660, slice thickness of 1.3 mm, and scanning time of 2 minutes 57 seconds per acquisition. Gadolinium contrast material (Omniscan before November 2010; gadoteridol [ProHance, Bracco Diagnostics]

from November 2010 through May 2013) was power-injected after the first acquisition (0.1 mmol/kg of body weight administered at 2 mL/s and followed by a 20-mL saline flush), and three contrast-enhanced acquisitions were performed. DWI was acquired using an echo-planar DWI sequence with parallel imaging (Sensitivity Encoding [SENSE], Philips Healthcare) and fat suppression (Spectral Attenuated Inversion Recovery [SPAIR], Philips Healthcare), a reduction factor of 3, TR/TE of 5336/61, 2 signal averages, FOV of 36 × 36 cm, matrix size of 240 × 240, 30 slices, slice thickness of 5 mm, and gap of 0 mm. Diffusion gradients were applied in six directions with diffusion sensitizations (b values) of 0, 100, and 800 s/mm^2; the scanning time was 3 minutes 28 seconds.

Unblinded Assessment of Lesion Features on DWI

Quantitative DWI measures——DW images were independently analyzed by a senior radiology resident who was not blinded to patient characteristics in the medical record or the DCE-MR images. Diffusion maps were created with in-house software written in Java language (Oracle) and incorporating an open-source image analysis tool (ImageJ, version 1.44, National Institutes of Health) [17, 19]. Combined isotropic DW images (S_{DWI}) were created as the geometric mean of individual DW images obtained using a b value of 600 or 800 s/mm^2, depending on the acquisition prototcol. ADC maps were calculated as follows:

$$ADC = -\left(\frac{1}{b}\right)\ln\frac{S_{DWI}}{S_o}$$

where S_0 is the T2-weighted reference image obtained using a b value of 0 s/mm^2.

An ROI was drawn around each lesion on DWI using the corresponding DCE images for reference. An ROI was also drawn in normal breast parenchyma in the ipsilateral breast. DWI signal intensity and ADC were measured for each lesion and for normal breast parenchyma as the mean of the voxel values within each ROI. The contrast-to-noise ratio (CNR) between the lesion and normal tissue on DWI was calculated as previously described [17, 20], using the following equation:

$$CNR = \frac{\mu_t - \mu_n}{\sqrt{\sigma_t^2 + \sigma_n^2}}$$

where μ_t and μ_n are the mean DWI signal intensity values for the tumor and normal fibroglandular tissue ROIs, respectively, and σ_t and σ_n are the corresponding respective SDs. A CNR of greater than 0 indicates higher DWI signal intensity in a lesion compared with normal tissue.

Visual conspicuity scores on DWI——The visual conspicuity of each lesion on DWI was graded separately by a board-certified radiologist with fellowship training in breast imaging and a senior radiology resident after completion of the reader study, which we discuss later. The two graders were not blinded to the medical record or to other imaging findings so that every lesion could be correctly identified and evaluated. Lesions were identified on DWI by referencing the DCE-MR images and corresponding imaging reports.

Lesions were graded according to both signal intensity strength and appearance using the following 5-point scale, which was used in a prior study [21]: 1, isointensity of the lesion to normal fibroglandular tissue; 2, nonlocalized mild-to-moderate signal intensity with an indistinct margin; 3, localized mild-to-moderate signal intensity; 4, nonlocalized strong signal intensity with an indistinct margin; and 5, localized strong signal intensity. A score of 3 or greater was considered visually distinguishable on DWI for analyses.

Blinded Assessment of Unenhanced MRI

Unenhanced MR images were interpreted by three fellowship-trained breast imagers with 4–6 years of breast MRI experience who were blinded to both DCE-MRI and clinical findings to assess screening performance characteristics. Each reader independently evaluated the 48 studies in a randomized order on a PACS workstation using only the following sequences: DW images with corresponding ADC maps, FSE T2-weighted images, and unenhanced non-fat-suppressed T1-weighted images. The readers were given instructions about how to interpret each study on the basis of the presence of a unique area of high signal intensity on DWI, the morphology and signal intensity of the finding on T2-weighted imaging, and the signal intensity of the finding on ADC maps (Fig. 1). Readers categorized findings for each breast separately as positive or negative for malignancy. Readers did not know the numbers of positive and negative cases in the study cohort. After completion of the reader study, an experienced radiologist reviewed the readers' responses to subjectively assess the DCE-MRI characteristics of the cases with false-negative DWI findings and the cases with false-positive DWI findings.

Statistical Analyses

Differences in signal intensity on DWI and in measures of ADC values between lesions and normal tissue were assessed using the paired Wilcoxon signed rank test. Unblinded lesion conspicuity scores were classified as visually distinguishable (score ≥ 3) or as not distinguishable (score < 3), and the percentage agreement between the graders was calculated. Differences in CNRs and ADCs between distinguishable lesions and nondistinguishable lesions and associations of CNRs, ADCs, and visual conspicuity scores (averaged between graders) with patient and lesion characteristics were assessed using the Mann-Whitney U test.

For the blinded reader study, sensitivity, specificity, positive predictive value (PPV), negative predictive value (NPV), and accuracy were calculated for each reader. The characteristics of the true-positive and false-negative studies, including size, morphology, histology, and MRI protocol, were evaluated. Analyses were conducted using statistics software (JMP version 11, SAS Institute). Except where indicated, data are presented as medians and ranges. A p value of < 0.05 was considered statistically significant.

Results

The characteristics of the 48 patients (24 patients with mammographically occult cancer and 24 negative control subjects) are given in Table 1. The median age of the cancer cohort was 50.5 years (range, 31–75 years). Two patients in the cancer cohort were high-risk *BRCA1*

mutation carriers, whereas the remaining patients had a family or personal history of breast cancer. One patient had bilateral cancers, with a mammographically occult cancer in the left breast and a cancer in the right breast that was visible on mammography; thus, only the left breast with mammographically occult cancer was evaluated for this study. The 24 biopsy-proven breast malignancies included 16 invasive cancers and eight ductal carcinoma in situ (DCIS) cancers identified on screening MRI. The lesions ranged in size from 5 to 34 mm (median, 10 mm). Of the 16 invasive cancers, 14 were estrogen receptor (ER)–positive, 13 were progesterone receptor (PR)–positive, and one was ErbB-2 (also known as HER2/neu)–positive; most were ER-positive, PR-positive, and ErbB-2–negative (n = 13/16), and one was a triple receptor-negative cancer (ER-negative, PR-negative, ErbB-2–negative). Of the eight DCIS lesions, six were ER-positive. Both *BRCA1* mutation carriers had mammographically occult ER-negative breast cancers (one DCIS and one triple receptor-negative invasive ductal carcinoma) detected on screening MRI.

Unblinded Assessment of Lesion Features on DWI

Overall, the mammographically occult malignancies showed higher signal intensity on DWI than ipsilateral normal tissue ($p < 0.0001$); the median lesion CNR was 1.4 on DWI (range, −0.6 to 4.6). The ADCs of the lesions (median, 1.31×10^3 mm^2/s; range, 0.49–2.24×10^3 mm^2/s) were lower than the ADCs of the ipsilateral normal tissue (median, 1.79×10^3 mm^2/s; range, 1.33–$2.39 \times 1CT^3$ mm^2/s; $p < 0.0001$). The CNRs and ADCs of the lesions were not significantly associated with lesion size, type, or histology or with patient characteristics ($p > 0.05$ for each; Table 2). The CNRs tended to be higher with the 3-T protocol (b value = 800 s/mm^2) than with the 1.5-T protocol (b value = 600 s/mm^2), but the difference was not significant ($p = 0.17$). Furthermore, no significant differences in CNRs or ADCs were observed between invasive lobular carcinoma and invasive ductal carcinoma ($p > 0.05$).

The percentage of mammographically occult malignancies assessed as visually distinguishable on DWI, defined as a conspicuity score 3 or greater, was 71% (17/24) for grader 1 and 58% (14/24) for grader 2 (mean, 65%). When only invasive cancers were considered, the mean percentage of malignancies assessed as visually distinguishable was 69% (11/16). Grader classifications (visually distinguishable vs not distinguishable) were in agreement for 19 of 24 lesions (79%). Grader scores were averaged for further analysis, and the results are reported in Table 2. The median lesion conspicuity score was 4 (range, 1–5); scores tended to be higher for masses than for nonmasses and to be higher for invasive cancers than for DCIS lesions, although the differences were not significant ($p > 0.05$). Figures 2 and 3 show examples of mammographically occult lesions with high and very high DWI conspicuity scores. Figure 4 shows an example of a mammographically occult lesion with a low DWI conspicuity score. There were no significant differences in conspicuity scores with respect to any of the assessed patient or imaging characteristics. Malignancies deemed distinguishable on visual assessment (conspicuity score ≥ 3) generally showed a higher CNR and a lower ADC than those deemed not distinguishable (Fig. 5), but the differences were not significant ($p = 0.07$ and 0.11, respectively).

Blinded Assessment of Unenhanced MRI

Three readers blinded to DCE and clinical findings separately evaluated the 48 studies for the presence of malignancy on unenhanced MRI. The performance of the three readers is summarized in Table 3. The mean sensitivity was 45% (range, 38–54%); mean specificity, 91% (90–93%); mean PPV, 62% (56–72%); and mean NPV, 83% (81–86%). The mean overall interpretive accuracy of the three readers was 79% (77–83%).

Of the 24 mammographically occult cancers, 16 (67%) were identified by at least one reader, 11 (46%) by at least two readers, and five (21%) by all three readers. Of the 11 cancers detected by two or more readers, nine were masses and two were areas of nonmass enhancement, and seven were imaged at 3 T. The median size of the cancers detected by two or more readers was 11.5 mm (range, 6–34 mm). Two lesions were invasive ductal carcinomas, four were invasive lobular carcinomas, one was a malignant phyllodes tumor, and four were DCIS lesions. Figure 6 shows an example of a cancer identified in this study that presented as a mass on DWI, and Figure 7 shows an example of a cancer identified in this study that presented as a nonmass on DWI. Figure 8 shows a benign mass correctly classified by all three readers.

Eight of the 24 cancers were missed by all readers, including four invasive ductal carcinomas, one invasive lobular carcinoma, and three DCIS lesions. The median size of the missed cancers was 12 mm (range, 6–26 mm); six presented as masses and two as nonmasses. Four of the missed cancers were imaged at 3 T and four at 1.5 T. Figure 9 shows a 7-mm invasive ductal carcinoma that was not identified by any of the readers. On average, readers incorrectly classified six of 71 negative breasts as positive for malignancy, resulting in 91% specificity. False-positive cases included a range of features on retrospective review, including a focal benign abnormality (e.g., fibroadenoma or proteinaceous cyst), imaging susceptibility-based artifact, and asymmetric elevated signal intensity on DWI due to prior treatment of the contralateral breast or to other factors. Examples of false-positive DWI findings are shown in Figures 10 and 11.

Discussion

The results of our study suggest that DWI may have promise as a rapid unenhanced technique for supplemental screening after mammography in women with dense breasts. We found that mammographically occult malignancies typically exhibited more restricted diffusion than the surrounding breast tissue, showing higher signal intensity on DWI and a lower ADC by quantitative assessment, and that 65% of the cancers were visually distinguishable from normal tissue on DWI. A blinded reader study with three independent readers showed that unenhanced MRI with DWI achieved 45% sensitivity and 91% specificity for detecting these challenging mammographically occult breast cancers.

Because approaches to patient care are increasingly tailored to individual factors, there is an urgent need to develop an efficient supplemental screening modality to address the known reduced sensitivity of mammography in women with dense breasts. Some investigators have proposed an expanded role for screening ultrasound in this population of women. The results of the large American College of Radiology Imaging Network (ACRIN) 6666 multicenter

trial [22] of intermediate-risk women and high-risk women with dense breasts indicated that ultrasound screening identified an additional four breast cancers per 1000 women screened and that a single contrast-enhanced MRI examination outperformed multiple years of ultrasound screening studies by detecting an additional 15 cancers per 1000 women over ultrasound and mammography combined. Additionally, although ultrasound is safe, it can be time-consuming and associated with very low specificity when used as a screening examination [8]. Contrast-enhanced MRI has the highest sensitivity for detecting cancers in dense breasts, but barriers to the widespread use of breast MRI include high cost, relatively lengthy scanning time, and contraindications related to the administration of gadolinium-based contrast material. Abbreviated breast MRI has been proposed as a possible faster and more cost-effective alternative [23], but this examination still does not address the safety issues associated with gadolinium contrast administration [24, 25]. Thus, a rapid unenhanced imaging approach that more closely approximates the performance of DCE-MRI in women with dense breasts without the poor specificity of ultrasound would provide high clinical value.

Our study is unique because it includes only cancers that were not detected on concurrent mammography in women with dense breasts, so these cancers would otherwise have been missed without supplemental screening. From the ACRIN 6666 trial [22] data, we estimate that the 45% sensitivity in our study would translate to the detection of eight additional cancers per 1000 women (estimated by 0.45 × 18/1000 added yield for DCE-MRI over mammography alone in ACRIN 6666 trial). This number of additional cancers detected exceeds the supplemental benefit of ultrasound after mammography (four additional cancers detected per 1000 women) with the potential advantage of higher specificity and higher PPV, which are especially important given concerns related to false-positive examinations associated with ultrasound screening.

The estimated sensitivity in our study (mean, 45%) is lower than the sensitivities reported in previous DWI studies (range, 50–94%) [12–14, 26–29]; however, this difference in results can be explained by critical differences in study design. Only a handful of the prior studies reporting DWI sensitivity incorporated a blinded reader study with negative control subjects to evaluate the performance for detecting cancer in a screening scenario, and the reported sensitivities for those studies ranged from 50% to 78% [12– 14]. Furthermore, our study was specifically designed to assess the added value of DWI to screening mammography in women with dense breasts. Therefore, in contrast to the prior reader studies, we included only cancers that were clinically and mammographically occult. The cancers in our study tended to be smaller (median size, 14 mm) than the cancers in prior reader studies (average size, = 20 mm [13, 14]), which may have reduced the detectability of the cancers in our study on DWI. Also, prior DWI reader studies included patients with known cancers that had been initially diagnosed by clinical examination, mammography, or ultrasound or had been previously biopsied, another factor that may have influenced lesion detectability because of the presence of marker clips and postbiopsy changes [12, 13]. Finally, we did not exclude any cases on the basis of the variable quality of the DW images with respect to common issues in breast DWI (e.g., fat suppression, signal-to-noise ratio, distortion) so as not to introduce bias, whereas other studies excluded up to 15% of lesions because of poor fat saturation or other factors [12, 26, 28].

Our study has several limitations. The DWI protocols at 3- and 1.5-T field strengths used different maximum b values; thus, we could not separate the effects of field strength and b value on conspicuity. For practicality in performing the reader study, we used scanner-generated isotropic DW images and ADC maps with default settings and without registration to correct for eddy current or motion artifacts, which may have reduced lesion conspicuity compared with the offline processing that was used for the unblinded analysis. In all cases, DWI was performed at the end of the MRI examination, after DCE-MRI, according to our institutional clinical breast MRI protocol. It is possible that signal intensity on DWI could be affected by residual circulating gadolinium, although we have previously shown no significant effect on breast tumor ADC measures using our imaging protocol [19]. Only BI-RADS 1 or 2 (control cohort) and true-positive BI-RADS 4 or 5 (cancer cohort) breast MRI examinations were included. Thus, this study was not designed to evaluate whether DWI might detect some cancers not visualized using DCE-MRI and also may underestimate the false-positive rate of DWI in the presence of BI-RADS 3 (probably benign) and false-positive BI-RADS 4 or 5 lesions. Readers were not provided with patient medical history or other imaging studies, which may have affected the interpretations. Finally, our study evaluated women with an elevated lifetime risk for breast cancer. Therefore, additional studies to determine the feasibility of using DWI for the target population of women with dense breasts but no other risk factors and to compare the performance of DWI with that of screening ultrasound in intermediate-risk women would greatly benefit the current debate on appropriate supplemental screening, if any, in the inter-mediate-risk population.

Further investigation of an unenhanced method of MRI screening is timely. Possible long-term health effects related to gadolinium administration (e.g., nephrogenic systemic fibrosis) were first identified in 2006, nearly 20 years after initial commercialization [30, 31]. More recently, gadolinium was reported to cross the blood-brain barrier and deposit in neural tissues in a dose-dependent manner [32]. This initial observation was subsequently confirmed by multiple clinical studies [25, 33–39], and the U. S. Food and Drug Administration is actively investigating the possible health associated with repeated gadolinium use [40]. The emerging data indicating a dose-dependent relationship between gadolinium administration and accumulation in the brain provides additional incentive to discover alternative screening methods for women at high risk for breast cancer, many of commence screening in their 20s and continue yearly without clear guidelines for cessation.

Our study highlights several areas of focus for future work to improve the sensitivity of DWI for detecting mammographically occult cancer in women with dense breasts. In particular, the optimal diffusion sensitization for lesion conspicuity may be greater than either b value used in this study [9, 20, 41, 42], and alternative approaches to increase DWI spatial resolution and reduce spatial distortions could further improve the detection of small lesions [43, 44]. With respect to the DWI interpretation process, refinements to the interpretation algorithms along with new computer-aided assessment tools to highlight suspicious features and combined presentation of ADC maps with DW images, such as a color-overlay scheme, may further improve reader performance.

In conclusion, the results of this study suggest that the addition of a rapid unenhanced MRI examination with DWI to conventional mammography screening could potentially identify a

significant number of mammographically occult cancers in women with dense breasts. Future work, including further optimization of the DWI approach and multicenter prospective screening trials, is warranted to better determine the value of unenhanced breast MRI with DWI as a supplemental screening tool.

Acknowledgments

Supported by grant R01-CA151326 from the National Institutes of Health and a grant from the Wings of Karen Foundation.

References

1. Saslow D, Boetes C, Burke W, et al.; American Cancer Society Breast Cancer Advisory Group. American Cancer Society guidelines for breast screening with MRI as an adjunct to mammography. CA Cancer J Clin 2007; 57:75–89 [Erratum in CA Cancer J Clin 2007: 57:185] [PubMed: 17392385]
2. DeMartini W, Lehman C, Partridge S. Breast MRI for cancer detection and characterization: a review of evidence-based clinical applications. Acad Radiol 2008; 15:408–416 [PubMed: 18342764]
3. Byrne C, Schairer C, Wolfe J, et al. Mammographic features and breast cancer risk: effects with time, age, and menopause status. J Natl Cancer Inst 1995; 87:1622–1629 [PubMed: 7563205]
4. McCormack VA, dos Santos Silva I. Breast density and parenchymal patterns as markers of breast cancer risk: a meta-analysis. Cancer Epidemiol Biomarkers Prev 2006; 15:1159–1169 [PubMed: 16775176]
5. Pettersson A, Graff RE, Ursin G, et al. Mammographic density phenotypes and risk of breast cancer: a meta-analysis. J Natl Cancer Inst 2014; 106: pii
6. Carney PA, Miglioretti DL, Yankaskas BC, et al. Individual and combined effects of age, breast density, and hormone replacement therapy use on the accuracy of screening mammography. Ann Intern Med 2003; 138:168–175 [PubMed: 12558355]
7. Lee Cl, Cevik M, Alagoz O, et al. Comparative effectiveness of combined digital mammography and tomosynthesis screening for women with dense breasts. Radiology 2015; 274:772–780 [PubMed: 25350548]
8. Sprague BL, Stout NK, Schechter C, et al. Benefits, harms, and cost-effectiveness of supplemental ultrasonography screening for women with dense breasts. Ann Intern Med 2015; 162:157–166 [PubMed: 25486550]
9. Partridge SC, McDonald ES. Diffusion weighted magnetic resonance imaging of the breast: protocol optimization, interpretation, and clinical applications. Magn Reson Imaging Clin N Am 2013; 21:601–624 [PubMed: 23928248]
10. Woodhams R, Matsunaga K, Iwabuchi K, et al. Diffusion-weighted imaging of malignant breast tumors: the usefulness of apparent diffusion coefficient (ADC) value and ADC map for the detection of malignant breast tumors and evaluation of cancer extension. J Cornput Assist Tomogr 2005; 29:644–649
11. Partridge SC, Demartini WB, Kurland BF, Eby PR, White SW, Lehman CD. Differential diagnosis of mammographically and clinically occult breast lesions on diffusion-weighted MRI. J Magn Reson Imaging 2010; 31:562–570 [PubMed: 20187198]
12. Kazama T, Kuroki Y, Kikuchi M, et al. Diffusion-weighted MRI as an adjunct to mammography in women under 50 years of age: an initial study. J Magn Reson Imaging 2012; 36:139–144 [PubMed: 22359367]
13. Trimboli RM, Verardi N, Cartia F, Carbonaro LA, Sardanelli F. Breast cancer detection using double reading of unenhanced MRI including T1-weighted, T2-weighted STIR, and diffusion-weighted imaging: a proof of concept study. AJR 2014; 203:674–681 [PubMed: 25148175]
14. Yabuuchi H, Matsuo Y, Sunami S, et al. Detection of non-palpable breast cancer in asymptomatic women by using unenhanced diffusion-weighted and T2-weighted MR imaging: comparison with

mammography and dynamic contrast-enhanced MR imaging. Eur Radiol 2011; 21:11–17 [PubMed: 20640898]

15. Morris EA, Comstock CE, Lee CH, et al. ACR BI-RADS magnetic resonance imaging. In: D'Orsi CJ, Sickles EA, Mendelson EB, et al. ACR BI-RADS Atlas, Breast Imaging Reporting and Data System. Reston, VA: American College of Radiology, 2013
16. American College of Radiology website. Breast magnetic resonance imaging program requirements, www.acr.org/~/media/ACR/Documents/Accreditation/BreastMRI/Requirements.pdf. Updated July 31, 2015. Accessed April 8, 2016
17. Parsian S, Rahbar H, Allison KH, et al. Nonmalignant breast lesions: ADCs of benign and high-risk subtypes assessed as false-positive at dynamic enhanced MR imaging. Radiology 2012; 265:696–706 [PubMed: 23033500]
18. McDonald ES, Schopp JG, Peacock s, et al. Diffusion-weighted MRI: association between patient characteristics and apparent diffusion coefficients of normal breast fibroglandular tissue at 3 T. AJR 2014; 202:(web)W496–W502 [PubMed: 24758685]
19. Nguyen VT, Rahbar H, Olson ML, Liu CL, Lehman CD, Partridge SC. Diffusion-weighted imaging: effects of intravascular contrast agents on apparent diffusion coefficient measures of breast malignancies at 3 tesla. Magn Reson Imaging 2015; 42:788–800
20. Bogner W, Gruber S, Pinker K, et al. Diffusion-weighted MR for differentiation of breast lesions at 3.0 T: how does selection of diffusion protocols affect diagnosis? Radiology 2009; 253:341–351 [PubMed: 19703869]
21. Chen X, He XJ, Jin R, et al. Conspicuity of breast lesions at different b values on diffusion-weighted imaging. BMC Cancer 2012; 12:334 [PubMed: 22853049]
22. Berg WA, Zhang Z, Lehrer D, et al.; ACRIN 6666 Investigators. Detection of breast cancer with addition of annual screening ultrasound or a single screening MRI to mammography in women with elevated breast cancer risk. JAMA 2012; 307:1394–1404 [PubMed: 22474203]
23. Kuhl CK, Schrading S, Strobel K, Schild HH, Hilgers RD, Bieling HB. Abbreviated breast magnetic resonance imaging (MRI): first postcontrast subtracted images and maximum-intensity projection—a novel approach to breast cancer screening with MRI. J Clin Oncol 2014; 32:2304–2310 [PubMed: 24958821]
24. Kanal E, Tweedle MF. Residual or retained gadolinium: practical implications for radiologists and our patients. Radiology 2015; 275:630–634 [PubMed: 25942418]
25. Kanda T, Osawa M, Oba H, et al. High signal intensity in dentate nucleus on unenhanced T1-weighted MR images: association with linear versus macrocyclic gadolinium chelate administration. Radiology 2015; 275:803–809 [PubMed: 25633504]
26. Baltzer PA, Benndorf M, Dietzel M, Gajda M, Camara O, Kaiser WA. Sensitivity and specificity of unenhanced MR mammography (DWI combined with T2-weighted TSE imaging, ueMRM) for the differentiation of mass lesions. Eur Radiol 2010; 20:1101–1110 [PubMed: 19936758]
27. Kuroki-Suzuki S, Kuroki Y, Nasu K, Nawano S, Moriyama N, Okazaki M. Detecting breast cancer with non-contrast MR imaging: combining diffusion-weighted and STIR imaging. Magn Reson Med Sci 2007; 6:21–27 [PubMed: 17510539]
28. Wu LM, Chen J, Hu J, Gu HY, Xu JR, Hua J. Diffusion-weighted magnetic resonance imaging combined with T2-weighted images in the detection of small breast cancer: a single-center multiobserver study. Acta Radiol 2014; 55:24–31 [PubMed: 23878358]
29. Yoshikawa MI, Ohsumi S, Sugata S, et al. Comparison of breast cancer detection by diffusion-weighted magnetic resonance imaging and mammography. Radiat Med 2007; 25:218–223 [PubMed: 17581710]
30. Marckmann P Skov L, Rossen K, et al. Nephrogenic systemic fibrosis: suspected causative role of gadodiamide used for contrast-enhanced magnetic resonance imaging. J Am Soc Nephrol 2006; 17:2359–2362 [PubMed: 16885403]
31. Grobner T Gadolinium: a specific trigger for the development of nephrogenic fibrosing dermopathy and nephrogenic systemic fibrosis? Nephrol Dial Transplant 2006; 21:1104–1108 [PubMed: 16431890]
32. Kanda T, Ishii K, Kawaguchi H, Kitajima K, Takenaka D. High signal intensity in the dentate nucleus and globus pallidus on unenhanced T1-weighted MR images: relationship with increasing

cumulative dose of a gadolinium-based contrast material. Radiology 2014; 270:834–841 [PubMed: 24475844]

33. Robert P, Lehericy S, Grand S, et al. T1-weighted hypersignal in the deep cerebellar nuclei after repeated administrations of gadolinium-based contrast agents in healthy rats: difference between linear and macrocyclic agents. Invest Radiol 2015; 50:473–480 [PubMed: 26107651]
34. Kanda T, Fukusato T, Matsuda M, et al. Gadolinium-based contrast agent accumulates in the brain even in subjects without severe renal dysfunction: evaluation of autopsy brain specimens with inductively coupled plasma mass spectroscopy. Radiology 2015; 276:228–232 [PubMed: 25942417]
35. McDonald RJ, McDonald JS, Kallmes DF, et al. Intracranial gadolinium deposition after contrast-enhanced MR imaging. Radiology 2015; 275:772–782 [PubMed: 25742194]
36. Ramalho J, Castillo M, AlObaidy M, et al. High signal intensity in globus pallidus and dentate nucleus on unenhanced T1-weighted MR images: evaluation of two linear gadolinium-based contrast agents. Radiology 2015; 276:836–844 [PubMed: 26079490]
37. Radbruch A, Weber ling LD, Kieslich PJ, et al. Gadolinium retention in the dentate nucleus and globus pallidus is dependent on the class of contrast agent. Radiology 2015; 275:783–791 [PubMed: 25848905]
38. Quattrocchi CC, Mallio CA, Errante Y, et al. Gadodiamide and dentate nucleus T1 hyperintensity in patients with meningioma evaluated by multiple follow-up contrast-enhanced magnetic resonance examinations with no systemic interval therapy. Invest Radiol 2015; 50:470–472 [PubMed: 25756685]
39. Errante Y, Cirimele V, Mallio CA, Di Lazzaro V, Zobel BB, Quattrocchi CC. Progressive increase of T1 signal intensity of the dentate nucleus on unenhanced magnetic resonance images is associated with cumulative doses of intravenously administered gadodiamide in patients with normal renal function, suggesting dechelation Invest Radiol 2014; 49:685–690 [PubMed: 24872007]
40. U.S. Food and Drug Administration website. Gadolinium-based contrast agents for magnetic resonance imaging (KIRI): drug safety communication—EDA evaluating the risk of brain deposits with repeated use. www.fda.gov/Safety/MedWatch/SafetyInformation/SafetyAlertsforHumanMedicalProducts/ucm456012.htm. Accessed January 6, 2015
41. Kuroki Y, Nasu K. Advances in breast MRI: diffusion-weighted imaging of the breast. Breast Cancer 2008; 15:212–217 [PubMed: 18491206]
42. Woodhams R, Ramadan S, Stanwell P, et al. Diffusion-weighted imaging of the breast: principles and clinical applications. RadioGraphics 2011; 31:1059–1084 [PubMed: 21768239]
43. Singer L, Wilmes LJ, Saritas EU, et al. High-resolution diffusion-weighted magnetic resonance imaging in patients with locally advanced breast cancer. Acad Radiol 2012; 19:526–534 [PubMed: 22197382]
44. Wisner DJ, Rogers N, Deshpande VS, et al. High-resolution diffusion-weighted imaging for the separation of benign from malignant BI-RADS 4/5 lesions found on breast MRI at 3T. J Magn Reson Imaging 2014; 40:674–681 [PubMed: 24214467]

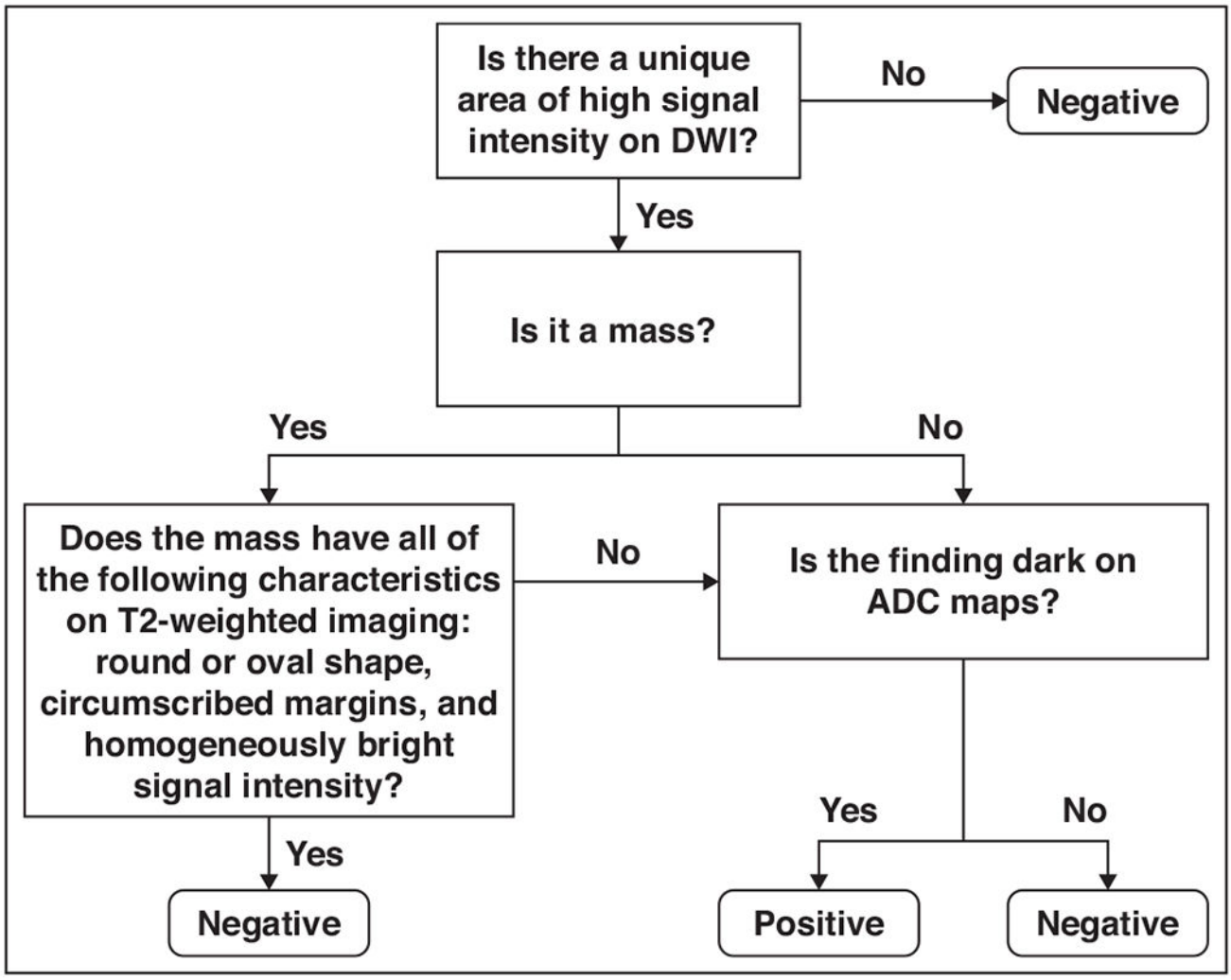

Fig. 1—.

Flowchart shows algorithm for DWI reader interpretation. Readers first evaluated images for unique area of high signal intensity on DWI. If no unique area of high signal intensity was present, study was reported as negative. If study was positive for unique high-signal-intensity area on DWI, reader categorized finding as mass or nonmass. If mass, reader evaluated T2-weighted sequence to determine whether any of following findings were present: round or oval shape, circumscribed margins, and homogeneously bright signal intensity. If mass met all of these criteria, it was reported as benign and classified as negative. If mass did not meet all of these criteria, reader assessed corresponding apparent diffusion coefficient (ADC) map. If mass was visually bright on ADC map (representing high diffusivity), it was reported as benign and classified as negative; if mass was dark on ADC map (representing low diffusivity), it was reported as positive. If finding was nonmass lesion, reader assessed ADC map as follows: If nonmass lesion was bright on ADC map, it was reported as benign and categorized as negative; if nonmass lesion was dark on ADC

map, it was reported as positive. As general rule, ADC value of ≤ 1.8×10^{-3} mm^2/s was considered suspicious for malignancy.

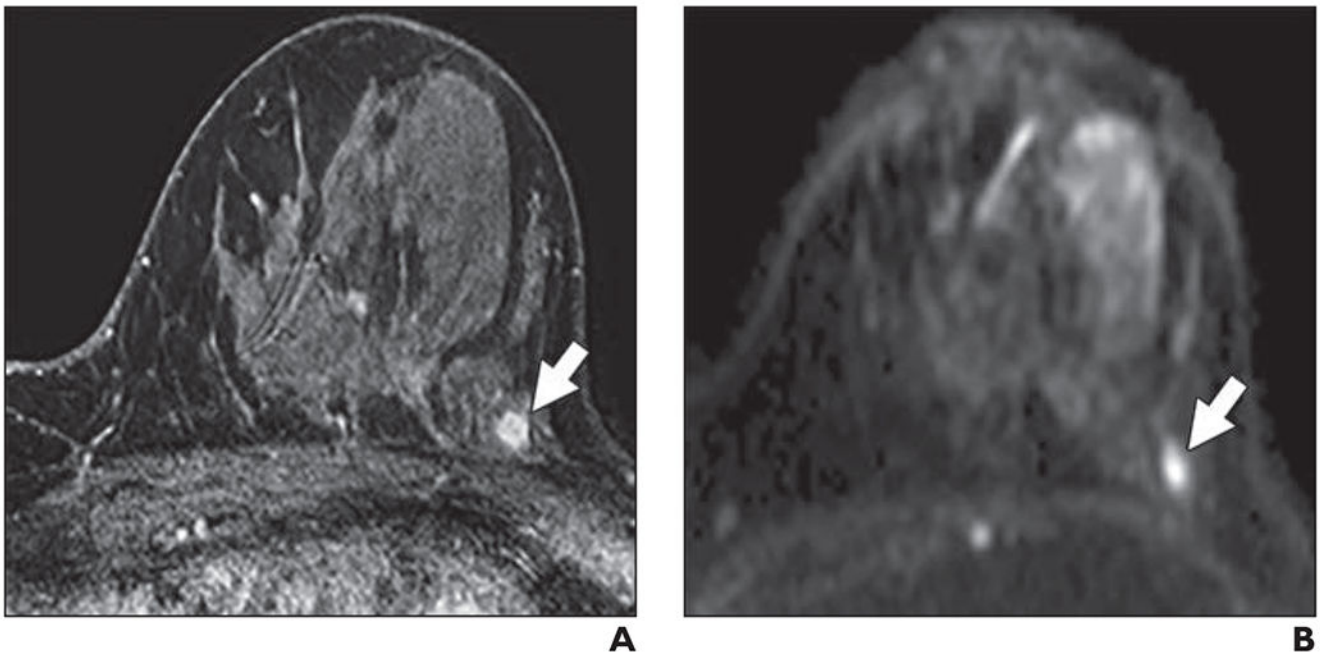

Fig. 2—.

58-year-old woman with dense breasts and mammographically occult invasive ductal carcinoma. This patient underwent high-risk screening MRI (3 T) because of personal history of right breast cancer.

A and **B,** Dynamic contrast-enhanced MR image (**A**) and DW image (**B**) show 5-mm mass (*arrow*). Mass was categorized as high conspicuity on DWI (mean conspicuity score = 4 of 5).

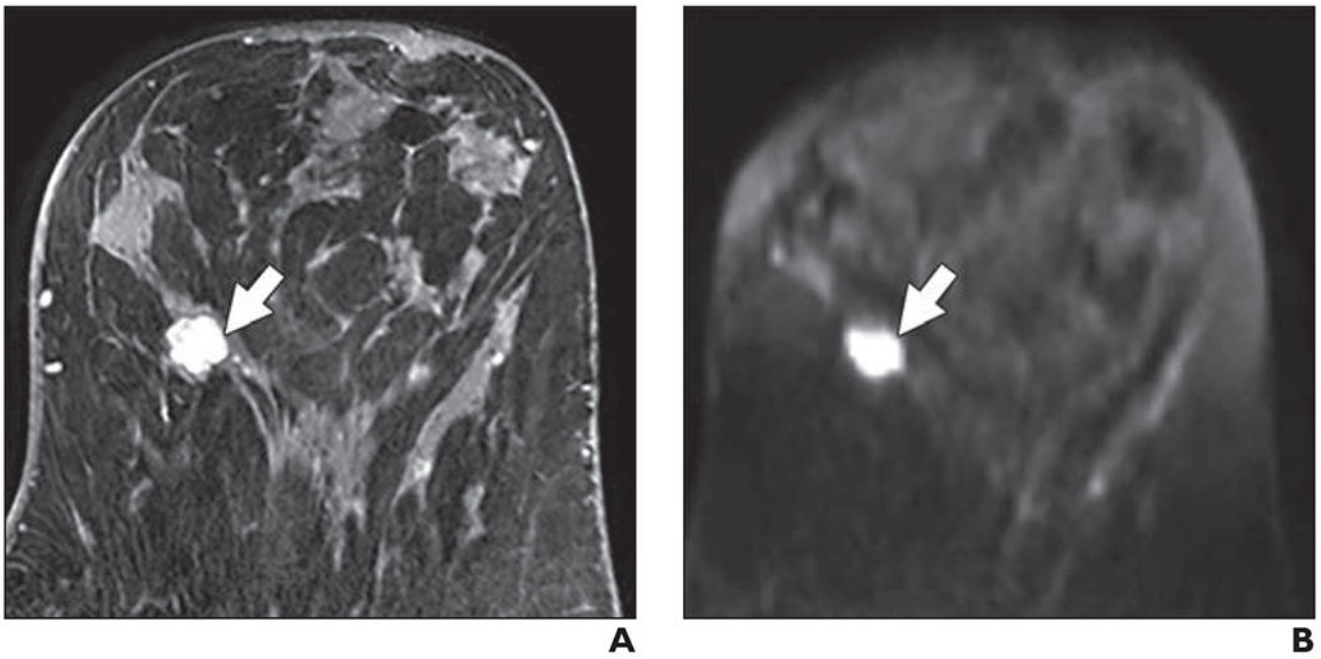

Fig. 3—.

58-year-old woman with dense breasts and mammographically occult malignant phyllodes tumor. Patient underwent high-risk screening MRI (3 T) because of strong family history of breast cancer.

A and **B,** Dynamic contrast-enhanced MR image (**A**) and DW image (**B**) show 13-mm mass (*arrow*). Mass was categorized as very high conspicuity on DWI (mean conspicuity score = 5 of 5).

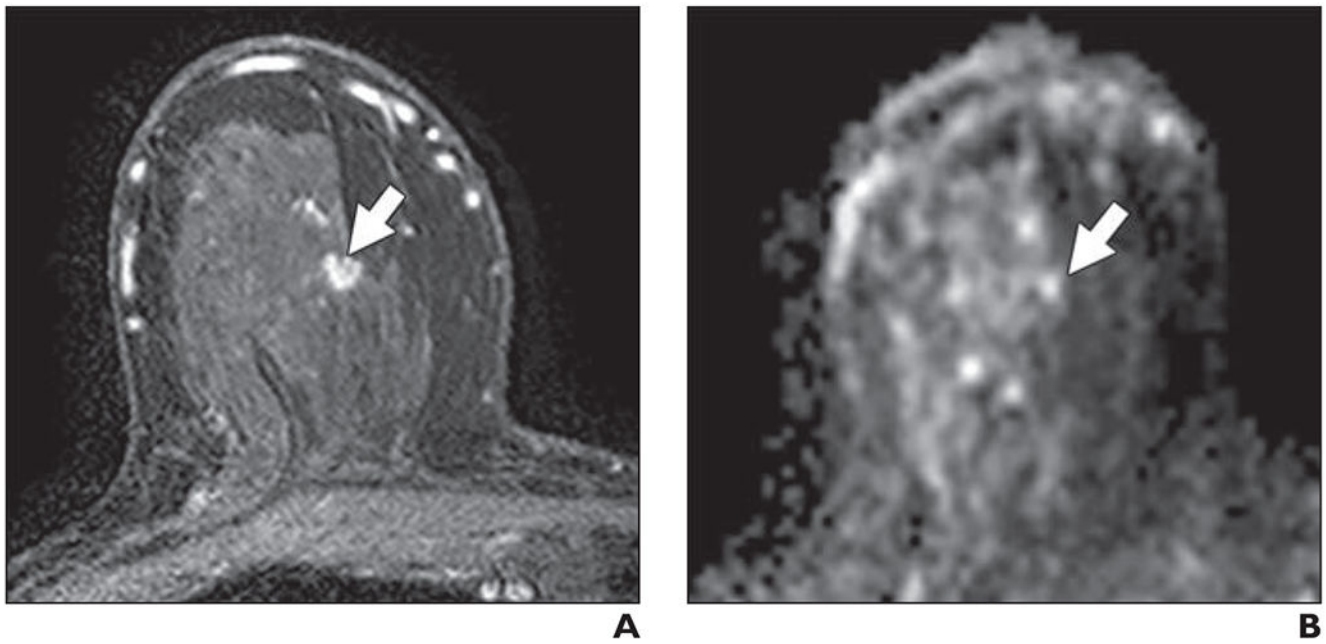

Fig. 4—.

68-year-old woman with dense breasts and mammographically occult invasive ductal carcinoma. This patient underwent high-risk screening MRI (3 T) because of personal history of breast cancer.

A and **B,** Dynamic contrast-enhanced MR image (**A**) and DW image (**B**) show 5-mm mass (*arrow*). Mass was categorized as very low conspicuity on DWI (mean conspicuity score = 1 of 5).

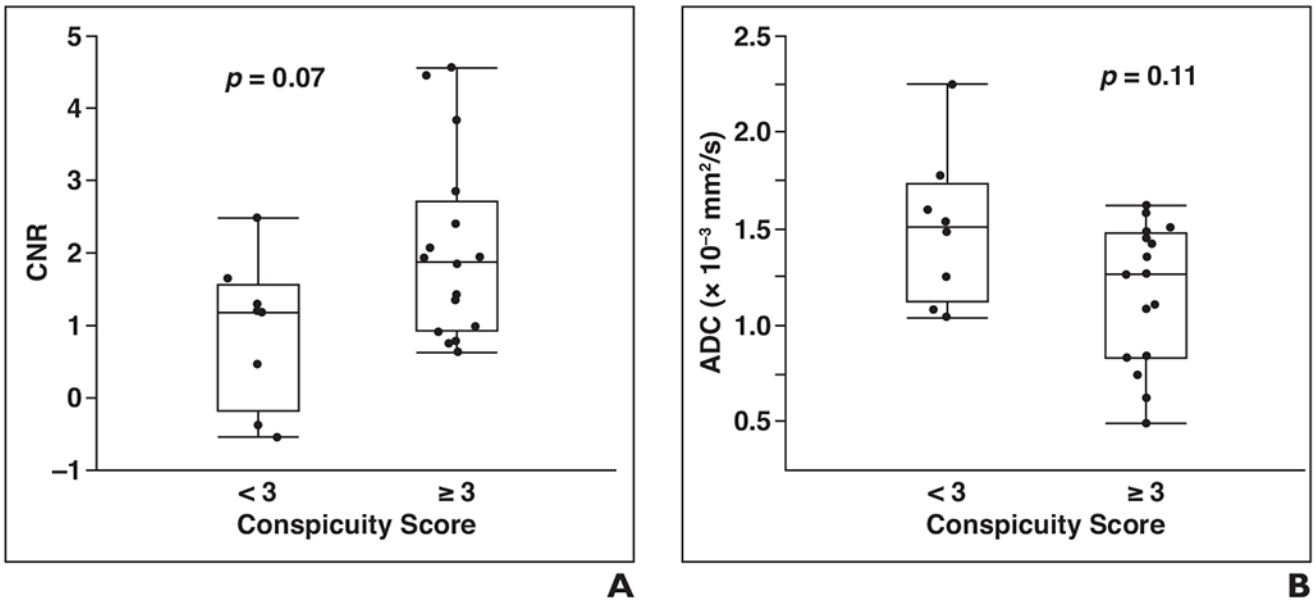

Fig. 5—.

Comparison of quantitative and qualitative features of breast lesions on DWI.

A, Graph shows that visually distinguishable lesions (conspicuity score ≥ 3; $n = 16$) tended to show higher contrast-to-noise ratio (CNR) on DWl than those that were not distinguishable (conspicuity score < 3; $n = 8$). Median CNR was 1.9 for visually distinguishable lesions versus 1.2 for lesions that were not distinguishable ($p = 0.07$). Upper and lower limits of boxes show 25th and 75th percentiles, respectively, and horizontal lines in middle of boxes show medians. Whiskers show range (minimum and maximum).

B, Graph shows that visually distinguishable lesions also tended to have lower apparent diffusion coefficient (ADC) values versus not distinguishable lesions, but difference was not significant. Median ADC is 1.26×10^{-3} mm^2/s for visually distinguishable lesions versus 1.51×10^{-3} mm^2/s for lesions that were not distinguishable ($p = 0.11$). Upper and lower limits of boxes show 25th and 75th percentiles, respectively, and horizontal lines in middle of boxes show medians. Whiskers show range (minimum and maximum).

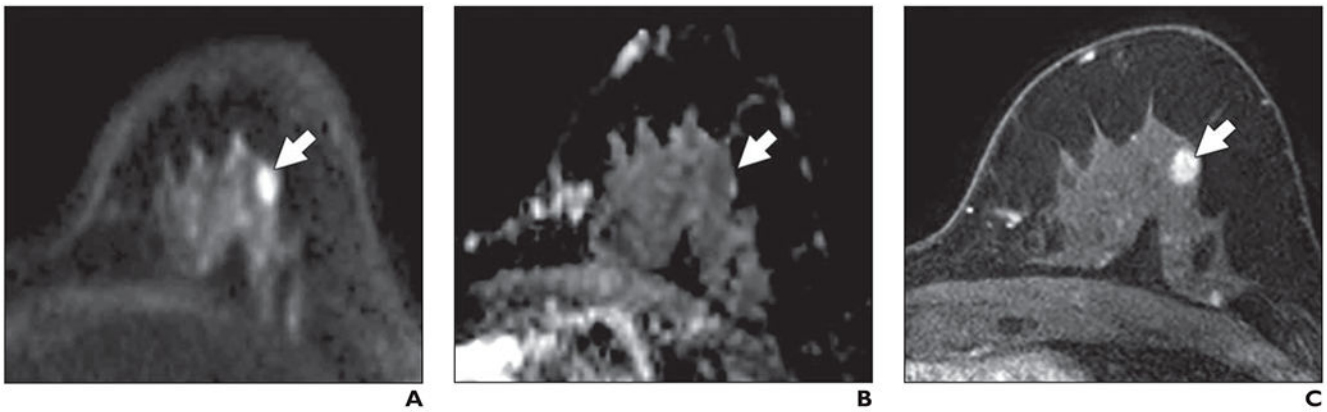

Fig. 6—.

58-year-old woman with dense breasts and mammographically occult invasive ductal carcinoma. Patient underwent high-risk screening MRI (3 T) because of strong family history of breast cancer. On DWI, this lesion received unblinded visual conspicuity score of 5 and was correctly identified in blinded reader study by two of three readers.

A, Axial DW image (b value = 800 s/mm^2) shows area of high signal intensity (*arrow*).

B, Apparent diffusion coefficient (ADC) map shows low diffusivity of lesion (*arrow*). ADC value is 1.45×10^{-3} mm^2/s.

C, T1-weighted dynamic contrast-enhanced MR image (provided here for reference, not provided to readers) shows enhancing 8-mm mass (*arrow*).

Fig. 7—.

74-year-old woman with dense breasts and mammographically occult high-grade ductal carcinoma in situ (DCIS). This patient underwent high-risk screening MRI (1.5 T) because of personal history of left breast cancer. On DWI, this lesion received unblinded visual conspicuity score of 4 and was correctly identified in blinded reader study by one of three readers.

A, Axial DW image (b value = 600 s/mm^2) shows nonmass area (*arrow*) is exhibiting high signal intensity.

B, Apparent diffusion coefficient (ADC) map shows low diffusivity of nonmass area (*arrow*). ADC value was 0.83×10^{-3} mm^2/s.

C, T1-weighted dynamic contrast-enhanced MR image (provided for reference, not provided to readers) shows 12-mm nonmass enhancement (*arrow*).

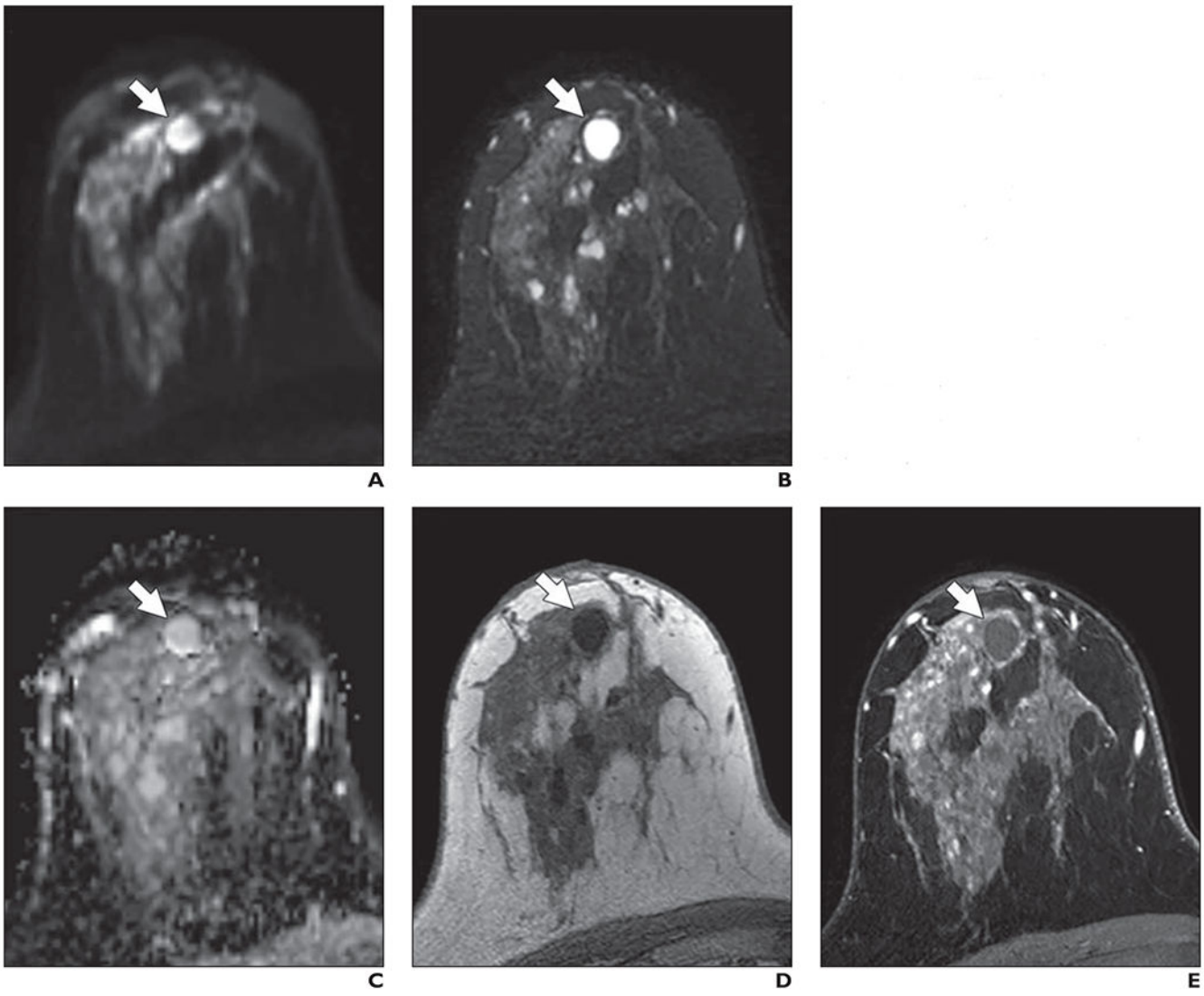

Fig. 8—.

49-year-old woman with dense breasts and benign mass. This patient underwent high-risk screening MRI (3 T) because of personal history of left breast cancer. On DWI, all three readers in blinded reader study correctly classified this breast as negative for malignancy.

A, Axial DW image (b value = 800 s/mm^2) shows mass with high signal intensity (*arrow*).

B, T2-weighted fast spin-echo image shows mass (*arrow*) meets all three criteria to be judged benign lesion: It is oval, has circumscribed margins, and is homogeneously bright.

C, Apparent diffusion coefficient (ADC) map shows high diffusivity of mass (*arrow*). ADC value is 2.11×10^{-3} mm^2/s.

D, Non-fat-suppressed T1-weighted fast gradient-echo image shows mass (*arrow*).

E, T1-weighted dynamic contrast-enhanced MR image (provided for reference, not provided to readers) shows no enhancement in mass (*arrow*).

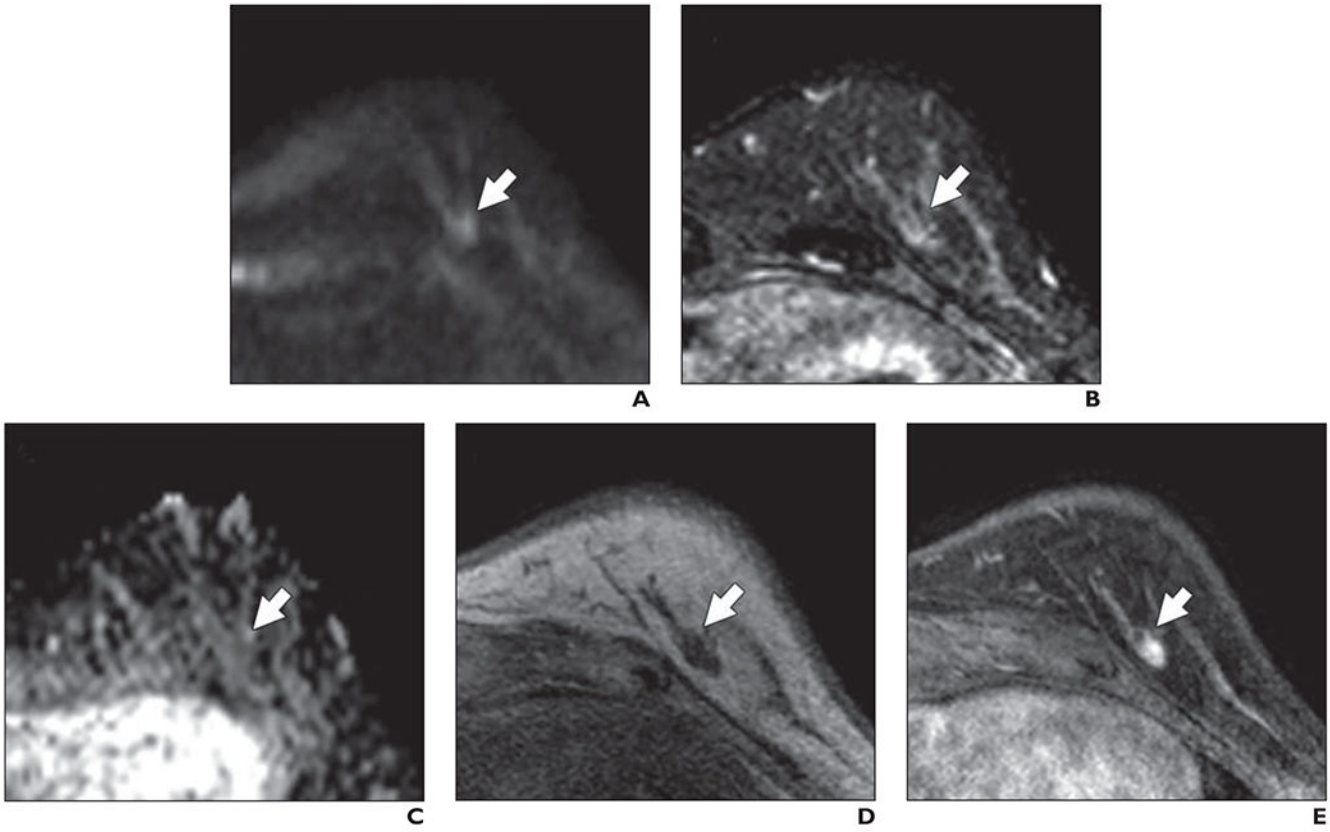

Fig. 9—.

53-year-old woman with dense breasts and mammographically occult invasive ductal carcinoma. This patient underwent high-risk screening MRI (3 T) because of personal history of high-risk lesion in right breast. On DWI, this lesion received unblinded visual conspicuity score of 1.5 and was missed by all three readers in blinded reader study.

A, Axial DW image (b value = 800 s/mm^2) shows area of mildly elevated signal intensity (*arrow*).

B. T2-weighted fast spin-echo image shows mass (*arrow*) is relatively isointense to normal fibroglandular tissue.

C, Apparent diffusion coefficient (ADC) map shows low diffusivity of mass (*arrow*). ADC value is 1.48×10^{-3} mm^2/s.

D, Non-fat-suppressed T1-weighted fast gradient-echo image shows mass (*arrow*).

E, Contrast-enhanced T1-weighted dynamic contrast-enhanced MR image (provided for reference, not provided to readers) shows 7-mm enhancing mass (*arrow*).

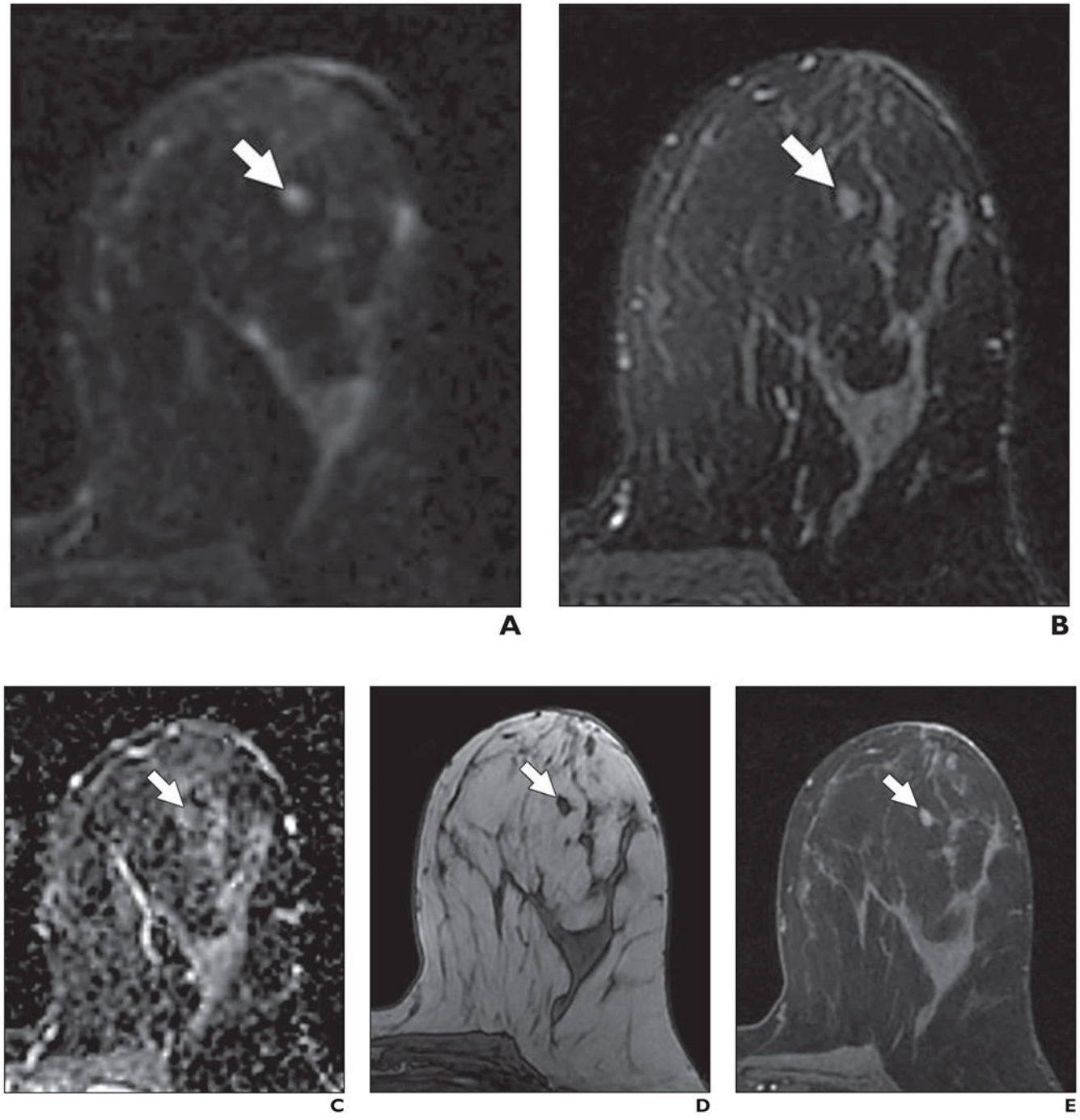

Fig. 10—.

44-year-old woman with heterogeneously dense breasts. This patient underwent high-risk screening MRI (1.5 T) because of strong family history of breast cancer. On DWI, all three readers in blinded reader study incorrectly classified this breast as positive for malignancy. **A,** Axial DW image (b value = 800 s/mm^2) shows focal mass (*arrow*) of elevated signal intensity identified by readers.

B, T2-weighted fast spin-echo image shows mass (*arrow*) is isointense to normal fibroglandular tissue. 44-year-old woman with heterogeneously dense breasts. This patient underwent high-risk screening MRI (1.5 T) because of strong family history of breast cancer. On DWI, all three readers in blinded reader study incorrectly classified this breast as positive for malignancy.

C, Apparent diffusion coefficient (ADC) map shows low diffusivity of mass (*arrow*). ADC value is 1.40×10^{-3} mm^2/s.

D, Non–fat-suppressed T1-weighted fast gradient-echo image shows mass (*arrow*).

E, T1-weighted dynamic contrast-enhanced MR image (provided for reference, not provided to readers) shows enhancing oval mass (*arrow*) with circumscribed margins and dark internal septation. Mass was categorized as benign finding on clinical dynamic contrast-enhanced MRI interpretation and likely represents benign fibroadenoma.

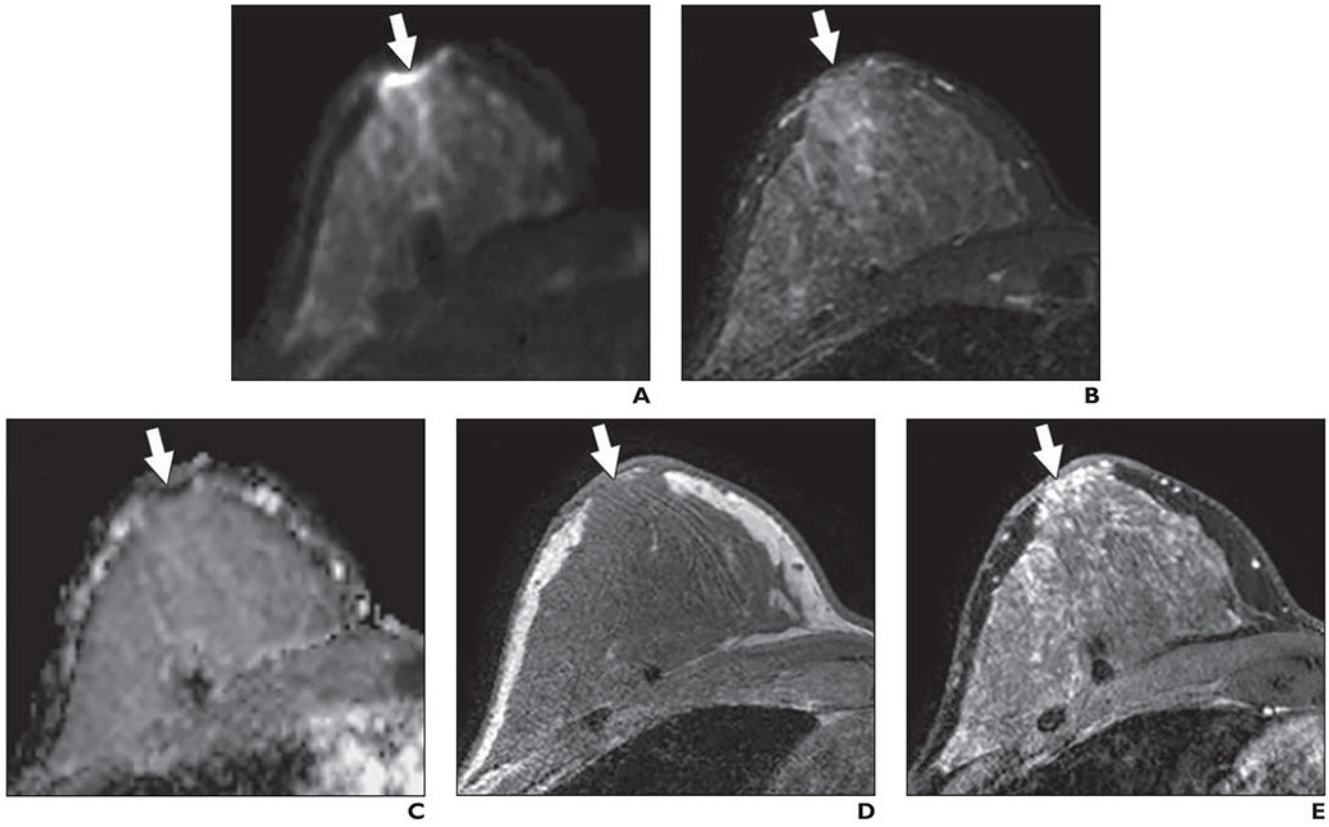

Fig. 11—.

54-year-old woman with dense breasts. This patient underwent high-risk screening MRI (3 T) because of high genetic risk (Ashkenazi Jewish heritage) and history of atypia in right breast. On DWI, one reader in blinded reader study incorrectly classified right breast as positive for malignancy.

A, Axial DW image (b value = 800 s/mm^2) shows area (*arrow*) of highly elevated signal intensity in subareolar region of right breast that was identified by one reader.

B, T2-weighted fast spin-echo image shows area (*arrow*) is isointense to adjacent fibroglandular tissue.

C, Apparent diffusion coefficient (ADC) map shows corresponding low diffusivity of area (*arrow*). ADC value is 1.20×10^{-3} mm^2/s.

D, Non–fat-suppressed T1-weighted fast gradient-echo image shows nothing abnormal in area (*arrow*). Comparison of this image with anatomic T2-weighted and T1-weighted images suggests presence of susceptibility-based distortion on DWI in nipple region. This artifact, which is caused by summation of mismapped pixels, is common in breast DWI and may explain elevated signal intensity identified at edge of breast.

E, T1-weighted dynamic contrast-enhanced MR image (provided for reference, not provided to readers) shows moderate but nonsuspicious background parenchymal enhancement (*arrow*).

TABLE 1:

Patient and Imaging Characteristics of the Cancer and Negative Cohorts[a]

Variable	Cancer Cohort (*n* = 24 Patients With Breast Cancer)	Negative Cohort (*n* = 24 Control Subjects)
Age (y), median (range)	50.5 (31-75)	51 (27-73)
Breast density, no. (%) of patients		
Heterogeneously dense	19 (79)	19 (79)
Extremely dense	5 (21)	5 (21)
Menopausal status, no. (%) of patients		
Premenopausal	10 (42)	12 (50)
Postmenopausal	14 (58)	12 (50)
Protocol, no. (%) of patients		
1.5 T	10 (42)	10 (42)
3 T	14 (58)	14 (58)
BI-RADS assessment based on conventional MRI, no. (%) of patients		
Category 1 (negative)	—	10 (42)
Category 2 (benign)	—	14 (58)
Category 3 (probably benign)	—	—
Category 4 (suspicious)	22 (92)	—
Category 5 (highly suggestive of malignancy)	2 (8)	—
Risk factors, no. (%) of patients		
Family history	13 (54)	24 (100)
Personal history	14 (58)	3 (13)
Positive for *BRCA1* mutation	2 (8)	4 (17)

Note—Dash indicates 0 patients.

[a]Control subjects were matched 1:1 with the patients with breast cancer for age, breast density, and MRI protocol.

TABLE 2:

Associations of DWI Lesion Features With Patient and Imaging Characteristics in 24 Women With Mammographically Occult Breast Cancer

Variable	No. of Patients	Conspicuity Score[a]	*p*[b]	CNR[a]	*p*[b]	ADC[a] (× 10^{-3} mm^2/s)	*p*[b]
Overall	24	4 (1-5)		1.4 (−0.6 to 4.6)		1.31 (0.49–2.24)	
Age (y)			0.40		0.82		0.86
<50	11	3.5 (1.5–4)		1.2 (−0.6 to 4.6)		1.26 (0.62–1.59)	
≥50	13	4 (1–5)		1.6 (−0.4 to 2.8)		1.35 (0.49–2.24)	
Menopausal status			0.27		0.84		0.50
Premenopausal	10	3.5 (1.5–4)		1.3 (−0.6 to 4.6)		1.45 (0.74–1.77)	
Postmenopausal	14	4 (1-5)		1.6 (−0.4 to 4.4)		1.26 (0.49–2.24)	
Lesion size (mm)			0.17		0.95		0.49
≤10	13	3.5 (1–5)		1.2 (0.5–4.6)		1.45 (0.49–1.77)	
>10	11	4 (1.5–5)		1.4 (−0.6 to 4.4)		1.25 (0.62–2.24)	
Lesion type			0.12		0.67		0.72
Mass	19	4 (1–5)		1.4 (−0.6 to 4.6)		1.42 (0.49–1.77)	
Nonmass enhancement	5	2.5 (1.5–4)		1.3 (−0.4 to 1.9)		1.25(0.83–2.24)	
Histology			0.25		0.44		0.88
IDC	10	4 (1–5)		1.1 (−0.6 to 4.6)		1.36 (0.49–1.59)	
ILC	5	4 (1.5–4)		2.5 (0.8–4.4)		1.08 (0.62–1.51)	
Phyllodes tumor	1	5		1.8		1.62	
DCIS	8	2.8 (1.5–4)		1.3 (−0.4 to 1.9)		1.30 (0.74–2.24)	
Protocol			0.38		0.17		0.93
1.5 T	10	3.5 (1.5–4)		1.2 (−0.6 to 2.1)		1.37 (0.49–1.77)	
3 T	14	4 (1–5)		1.9 (−0.4 to 4.6)		1.31 (0.62–2.24)	

Note—IDC = invasive ductal carcinoma, ILC = invasive lobular carcinoma, DCIS = ductal carcinoma in situ.

[a]Median (range).

[b]The *p* values were calculated using the Mann-Whitney *U* test; histology comparisons were performed for invasive tumors (i.e., IDC, ILC, malignant phyllodes tumor) versus noninvasive tumors (i.e., DCIS).

TABLE 3:

Performance of Blinded Readers Using Unenhanced MRI Screening Studies With DWI for Assessing 95 Breasts[a] of 48 Women[b]

Reader	Sensitivity (%)	Specificity (%)	PPV (%)	NPV (%)	Accuracy (%)
Reader 1	42 (10/24)	90 (64/71)	59 (10/17)	82 (64/78)	78 (74/95)
Reader 2	54 (13/24)	93 (66/71)	72 (13/18)	86 (66/77)	83 (79/95)
Reader 3	38 (9/24)	90 (64/71)	56 (9/16)	81 (64/79)	77 (73/95)
Mean reader performance	45	91	62	83	79

Note—Raw data (no. /total no.) are presented in parentheses. PPV = positive predictive value, NPV = negative predictive value.

[a]Only one breast of one patient was included in the analysis because she had non–mammographically occult disease in the contralateral breast.

[b]Twenty-four women with breast cancer and 24 control subjects who were matched 1:1 with the patients with breast cancer for age, breast density, and MRI protocol.